Available online at www.sciencedirect.com
ScienceDirect
Virology 375 (2008) 277–291
VIROLOGY
www.elsevier.com/locate/yviro

AcMNPV *ac143* (*odv-e18*) is essential for mediating budded virus production and is the 30th baculovirus core gene

Christina B. McCarthy, David A. Theilmann *

Pacific Agri-Food Research Centre, Agriculture and Agri-Food Canada, Summerland, British Columbia, Canada V0H 1Z0

Received 14 December 2007; returned to author for revision 2 January 2008; accepted 29 January 2008
Available online 6 March 2008

Abstract

Autographa californica multiple nucleopolyhedrovirus (AcMNPV) *ac143* (*odv-e18*) is a late gene that encodes for a predicted 9.6 kDa structural protein that locates to the occlusion derived viral envelope and viral induced intranuclear microvesicles [Braunagel, S.C., He, H., Ramamurthy, P., and Summers, M.D. (1996). Transcription, translation, and cellular localization of three *Autographa californica* nuclear polyhedrosis virus structural proteins: ODV-E18, ODV-E35, and ODV-EC27. Virology 222, 100–114.]. In this study we demonstrate that *ac143* is actually a previously unrecognized core gene and that it is essential for mediating budded virus production. To examine the role of *ac143* in the baculovirus life cycle, we used the AcMNPV bacmid system to generate an *ac143* knockout (KO) virus (AcBAC$^{ac142\text{REP}\text{-}ac143\text{KO}}$). Fluorescence and light microscopy showed that infection by AcBAC$^{ac142\text{REP}\text{-}ac143\text{KO}}$ is limited to a single cell and titration assays confirmed that AcBAC$^{ac142\text{REP}\text{-}ac143\text{KO}}$ was unable to produce budded virus (BV). Progression to very late phases of the viral infection was evidenced by the development of occlusion bodies in the nuclei of transfected cells. This correlated with the fact that viral DNA replication was unaffected in AcBAC$^{ac142\text{REP}\text{-}ac143\text{KO}}$ transfected cells. The entire *ac143* promoter, which includes three late promoter motifs, is contained within the *ac142* open reading frame. Different deletion mutants of this region showed that the integrity of the *ac142-ac143* core gene cluster was required for the bacmids to display wild-type patterns of viral replication, BV production and RNA transcription.

Keywords: *ac143* (*odv-e18*); *ac142*; Core gene; Cluster; BV; ODV

Introduction

Autographa californica multiple nucleopolyhedrovirus (AcMNPV) is the type species of the genus *Nucleopolyhedrovirus* of the family *Baculoviridae*. During the infection cycle, AcMNPV produces two structurally and functionally distinct enveloped virion phenotypes: occlusion derived virus (ODV) and budded virus (BV) (Theilmann et al., 2005). ODV are occluded in the nucleus in a protein matrix that forms polyhedra or occlusion bodies which are required for the horizontal transmission of the virus. The alkaline environment in the midgut lumen of the larva releases ODV from the occlusion bodies, enabling these viral particles to initiate primary infection of the mature columnar epithelial cells of the midgut. BV are produced when nucleocapsids bud through the plasma membrane of the midgut epithelial cells or other tissues to initiate secondary infections within the infected animal (Granados and Lawler, 1981; Keddie et al., 1989).

AcMNPV has a double-stranded DNA genome of approximately 134 kbp that contains 154 predicted open reading frames (ORFs) (Ayres et al., 1994). More than 40 baculovirus genomes have been completely sequenced to date and comparative analyses have reported that 29 core genes are conserved in all genomes and are therefore likely to serve essential roles in the baculovirus life cycle (Garcia-Maruniak et al., 2004; Herniou et al., 2003). Several of the core genes have a known function and are required for RNA transcription, DNA replication and as structural and auxiliary proteins. The function of seven core genes: *38K* (*ac98*), *p33* (*ac92*), *ac68*, *ac81*, *ac96*, *ac109*, and *ac115*, remains unknown (Herniou et al., 2003).

Various AcMNPV genes have been shown to affect the production of BV and ODV. Core genes *vp1054* (*ac54*) and *vlf-1*

* Corresponding author. Pacific Agri-Food Research Centre, Agriculture and Agri-Food Canada, Box 5000, Summerland, B.C., Canada V0H 1Z0. Fax: +1 250 494 7715.
E-mail address: TheilmannD@agr.gc.ca (D.A. Theilmann).

0042-6822/$ - see front matter Crown Copyright © 2008 Published by Elsevier Inc. All rights reserved.
doi:10.1016/j.virol.2008.01.039

(*ac77*) express nucleocapsid proteins that are structural components of both BV and ODV and are required for the assembly of nucleocapsids in the nucleus (Olszewski and Miller, 1997a; Vanarsdall et al., 2006; Yang and Miller, 1998). *Gp41* (*ac80*) is also a core gene that expresses an *O*-glycosylated protein which affects both BV and ODV but is only a structural component of ODV (Lee and Miller, 1979; Olszewski and Miller, 1997b; Yang and Miller, 1998). The nucleocapsid protein P78/83, associated with both BV and ODV, is essential for AcMNPV viability (Possee et al., 1991; Russell et al., 1997; Vialard and Richardson, 1993). The baculovirus core gene *38K* (*ac98*) has been shown to be essential for the formation of normal nucleocapsids, affecting both BV and ODV production, but it has not been shown to be a structural component of nucleocapsids (Wu et al., 2006). Recently, it was shown in two studies using AcMNPV gene knockout (KO) bacmids, that *ac142* is essential for BV and ODV production (McCarthy et al., 2008; Vanarsdall et al., 2007). In addition, it was shown that in the absence of *ac142*, bundles of nucleocapsids were unable to acquire the nuclear viral envelope and failed to form ODV. Failure to form ODV also resulted in the formation of occlusion bodies that were devoid of virions.

Intimately associated with *ac142* is *ac143* (*odv-e18*), a late gene that is transcribed from three conserved late promoter motifs A/T/GTAAG (DTAAG) contained within the *ac142* coding region. *Ac143* encodes a structural protein shown by immunoelectron microscopy and biochemical fractionation to be part of the AcMNPV ODV envelope (Braunagel et al., 1996). In addition, *ac143* has been predicted to form a dimer in infected cells and localizes to the viral induced intranuclear microvesicles prior to the envelopment of nucleocapsid bundles during the formation of ODV (Braunagel et al., 1996).

Predicted features for *ac143* include a transmembrane domain and an overlapping signal peptide in the N-terminus.

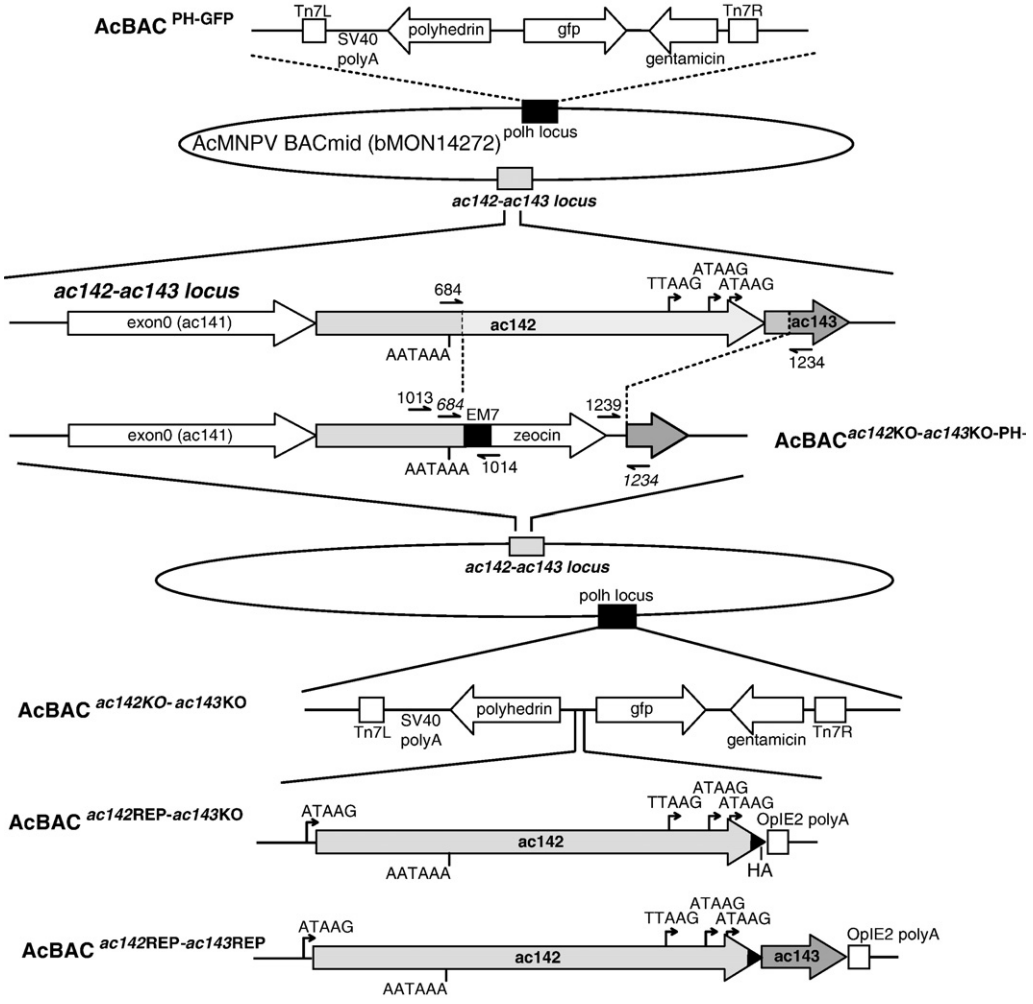

Fig. 1. Construction of *ac143* knockout, repair and positive control AcMNPV bacmids. Schematic diagram describing the construction of bacmids AcBAC$^{ac142\text{REP-}ac143\text{KO}}$, AcBAC$^{ac142\text{REP-}ac143\text{REP}}$ and AcBAC$^{\text{PH-GFP}}$. The *ac142-ac143* locus was partially deleted by replacement with an EM7-*zeocin* gene resistance cassette (amplified with primers 684 and 1234) *via* homologous recombination in *E. coli*, to generate AcBAC$^{ac142\text{KO-}ac143\text{KO-PH-}}$. The deletion did not affect the polyA signal for *exon0* (*ac141*) included in the *ac142* coding region. The deletion in the *ac142-ac143* locus was confirmed using primers 1013 and 1014; their relative positions are indicated. The lower part of the figure shows the genes inserted in the *polyhedrin* (polh) locus of AcBAC$^{ac142\text{KO-}ac143\text{KO-PH-}}$ by Tn7-mediated transposition to generate AcBAC$^{ac142\text{REP-}ac143\text{KO}}$ and AcBAC$^{ac142\text{REP-}ac143\text{REP}}$. The *ac142* ORF inserted into AcBAC$^{ac142\text{REP-}ac143\text{KO}}$ is driven by its own promoter and includes an in-frame C-terminal HA-epitope (indicated as a black triangle). The *ac142* and *ac143* ORFs inserted into AcBAC$^{ac142\text{REP-}ac143\text{REP}}$ are driven by their native promoters. The AcBAC$^{\text{PH-GFP}}$ bacmid was generated by insertion of the *polyhedrin* and *gfp* genes into the *polyhedrin* locus of bMON14272 bacmid.

In AcMNPV, *ac142* and *ac143* are contained within a region of the genome that is transcriptionally complex, the IE0 intron. Multiple transcripts, including spliced transcripts, are produced from this region both early and late in infection (Kovacs et al., 1991). Homologues of both genes have been identified in all lepidopteran and hymenopteran baculoviruses. However, in the dipteran baculovirus sequenced to date, homologues of *ac142* but not *ac143* have been identified (Afonso et al., 2001; Duffy et al., 2006; Garcia-Maruniak et al., 2004; Herniou et al., 2003; Jehle et al., 2006; Lauzon et al., 2004).

In this study we have investigated the role of *ac143* in AcMNPV replication by producing an *ac143* deletion mutant using the AcMNPV bacmid system. We discovered that *ac143* is essential for mediating budded virus production and that the *ac143* deletion mutant produces a single cell infection phenotype. Several different deletion mutants were generated to analyze the *ac143* promoter region. In each case, modification in this region affected *ac143* transcription and significantly decreased viral replication. In addition, we identify a homolog of *ac143* in *Culex nigripalpus* NPV (CuniNPV) which indicates that *ac143* is a baculovirus core gene.

Results

Generation of ac143 knockout and repair bacmids

Using the AcMNPV bMON14272 bacmid, a double *ac142-ac143* KO was generated through homologous recombination in *E. coli* as previously described (Fig. 1) (Datsenko and Wanner, 2000; Lin and Blissard, 2002). As the promoter of *ac143* is contained within the *ac142* ORF, to enable the analysis of both the *ac143* promoter and its function, an *ac143-ac142* double KO was generated (Fig. 1). The *ac142-ac143* KO left 521 bp of the 5' end of the *ac142* ORF intact to ensure that the *exon0*(*ac141*) polyA signal sequence contained in the *ac142* coding region was preserved (Fig. 1) (Braunagel et al., 1996; Dai et al., 2004; Harrison and Bonning, 2003). The complete *ac143* promoter and half of the *ac143* ORF were deleted and replaced with the EM7-*zeocin* resistance gene cassette (Fig. 1).

The resulting *ac142-ac143* KO bacmid, AcBAC$^{\text{-}ac142\text{KO-}ac143\text{KO-PH-}}$, was examined by PCR analysis (data not shown). To confirm the correct insertion of the *zeocin* gene cassette into the *ac142-ac143* locus, primer pairs 1013/1014 were used to examine the recombination junctions of the upstream flanking region (Fig. 1). The PCR results confirmed that the central region of the *ac142-ac143* locus had been deleted as expected (data not shown).

To establish the effect of a single *ac143* deletion on virus replication and to facilitate examination of virus infection, AcBAC$^{\text{-}ac142\text{KO-}ac143\text{KO-PH-}}$ was repaired with a previously described plasmid (McCarthy et al., 2008) containing *ac142*, *polyhedrin* and *gfp*, which were inserted into the *polyhedrin* locus of AcBAC$^{\text{-}ac142\text{KO-}ac143\text{KO-PH-}}$ by transposition (Fig. 1). This virus was named AcBAC$^{ac142\text{REP-}ac143\text{KO}}$. To rescue and confirm that the phenotype resulting from the *ac143* KO was not due to genomic effects, a bacmid repaired with both

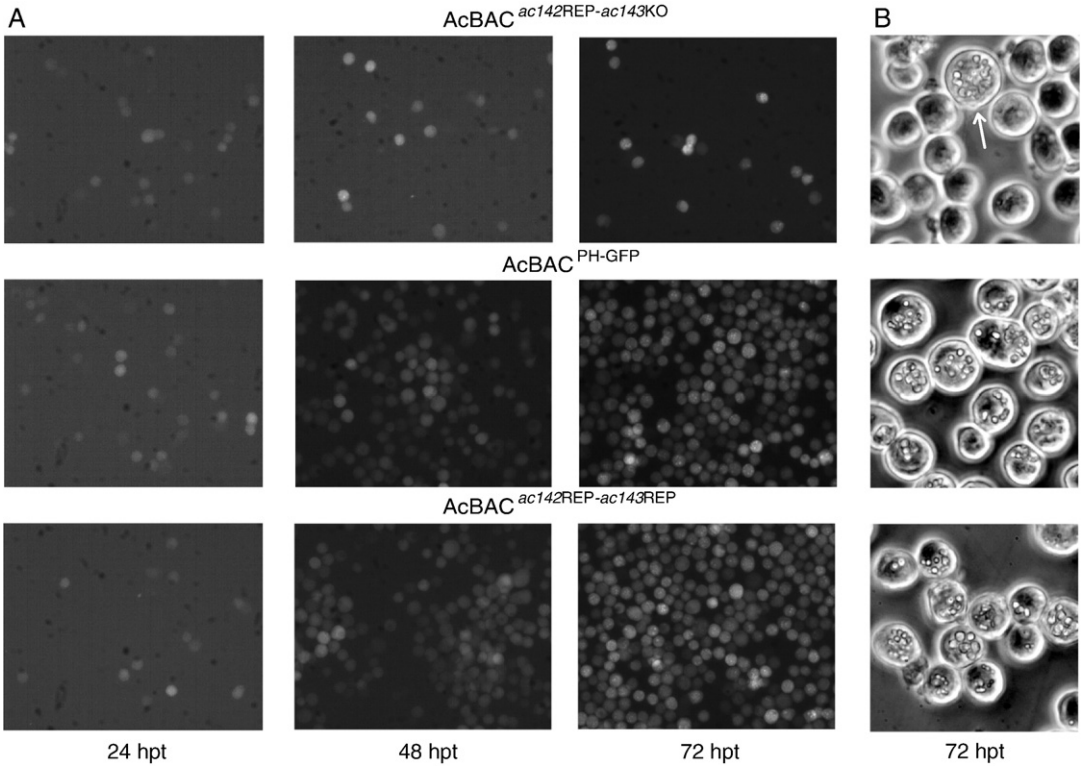

Fig. 2. Viral replication analysis of AcBAC$^{ac142\text{REP-}ac143\text{KO}}$, AcBAC$^{ac142\text{REP-}ac143\text{REP}}$ and AcBAC$^{\text{PH-GFP}}$-transfected cells. A) Fluorescence microscopy showing the progression of the infection in *Sf*9 cells transfected with AcBAC$^{ac142\text{REP-}ac143\text{KO}}$, AcBAC$^{ac142\text{REP-}ac143\text{REP}}$ and AcBAC$^{\text{PH-GFP}}$ at 24, 48, and 72 hpt. (B) Light microscopy of *Sf*9 cells transfected with AcBAC$^{ac142\text{REP-}ac143\text{KO}}$, AcBAC$^{ac142\text{REP-}ac143\text{REP}}$ and AcBAC$^{\text{PH-GFP}}$ at 72 hpt. The arrow indicates a single cell producing normal appearing occlusion bodies in AcBAC$^{ac142\text{REP-}ac143\text{KO}}$-transfected cells compared to AcBAC$^{ac142\text{REP-}ac143\text{REP}}$ and AcBAC$^{\text{PH-GFP}}$.

ac142 and *ac143*, AcBAC$^{ac142\text{REP-}ac143\text{REP}}$, was generated. AcBAC$^{ac142\text{REP-}ac143\text{REP}}$ contained *ac142* and *ac143*, expressed under the control of their native promoters, in addition to *polyhedrin* and *gfp* (Fig. 1). AcBAC$^{\text{PH-GFP}}$, which was used as a positive control, was constructed by transposing the *polyhedrin* and *gfp* genes into the *polyhedrin* locus of AcMNPV bacmid bMON14272 (Fig. 1). The resulting bacmids, AcBAC$^{ac142\text{REP-}ac143\text{KO}}$, AcBAC$^{ac142\text{REP-}ac143\text{REP}}$ and AcBAC$^{\text{PH-GFP}}$, were confirmed by PCR analysis (data not shown).

Analysis of AcBAC$^{ac142REP\text{-}ac143KO}$, AcBAC$^{ac142REP\text{-}ac143REP}$ and AcBAC$^{PH\text{-}GFP}$ replication in transfected Sf9 cells

To determine the effect of the *ac143* deletion on virus replication, *Sf*9 cells were transfected with AcBAC$^{ac142\text{REP-}ac143\text{KO}}$, AcBAC$^{ac142\text{REP-}ac143\text{REP}}$ and AcBAC$^{\text{PH-GFP}}$. As all the constructs express *gfp* under the control of the constitutive Op*M*NPV *ie1* promoter, transfected cells were monitored by fluorescence microscopy. No difference was observed among the three viruses at 24 h post-transfection (hpt), indicating comparable transfection efficiencies (Fig. 2A). By 48 and 72 hpt, AcBAC$^{ac142\text{REP-}ac143\text{KO}}$-transfected cells showed no increase in the number of infected cells (Fig. 2A), indicating that there was no spread of the virus beyond the initially transfected cells. This result suggested that AcBAC$^{ac142\text{REP-}ac143\text{KO}}$ was incapable of producing infectious BV. In contrast, by 48 hpt, fluorescence was observed in almost all AcBAC$^{\text{PH-GFP}}$ and AcBAC$^{ac142\text{REP-}ac143\text{REP}}$ transfected cells (Fig. 2A), indicating that both viruses were capable of generating infectious BV from the initial transfection and that the single cell phenotype observed was due to the *ac143* deletion.

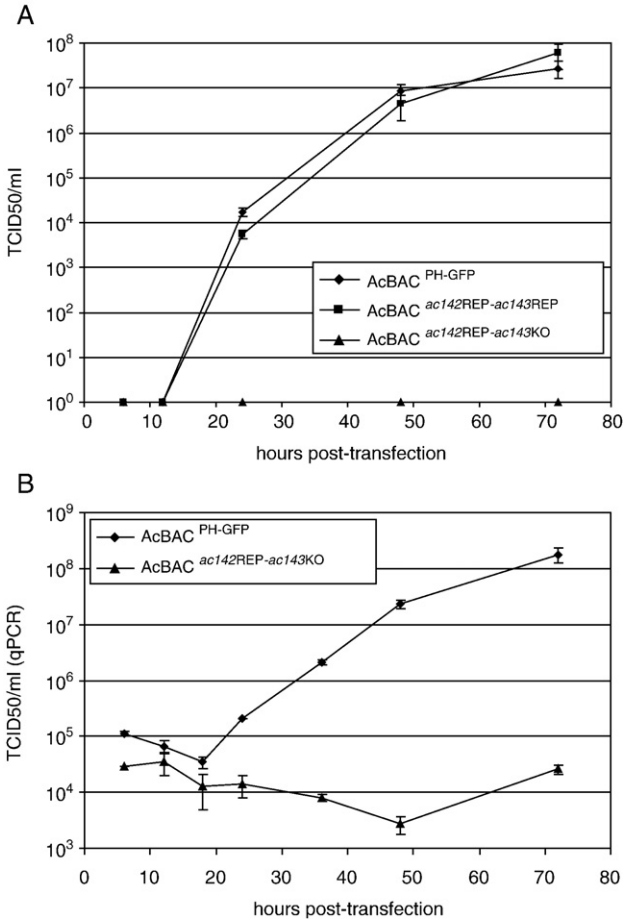

Fig. 3. Replication kinetics of *Sf*9 cells transfected with AcBAC$^{ac142\text{REP-}ac143\text{KO}}$, AcBAC$^{ac142\text{REP-}ac143\text{REP}}$ and AcBAC$^{\text{PH-GFP}}$. A) Virus growth curve determined by $TCID_{50}$ end-point dilution generated from *Sf*9 cells transfected with AcBAC$^{ac142\text{REP-}ac143\text{KO}}$, AcBAC$^{ac142\text{REP-}ac143\text{REP}}$ and AcBAC$^{\text{PH-GFP}}$. Each datum point represents the average titer derived from two independent $TCID_{50}$ assays. Error bars represent standard deviation. (B) Virus titer independent of viral infectivity was determined by qPCR analysis of supernatants of AcBAC$^{ac142\text{REP-}ac143\text{KO}}$ and AcBAC$^{\text{PH-GFP}}$-transfected *Sf*9 cells at the designated time-points. Error bars represent standard deviation.

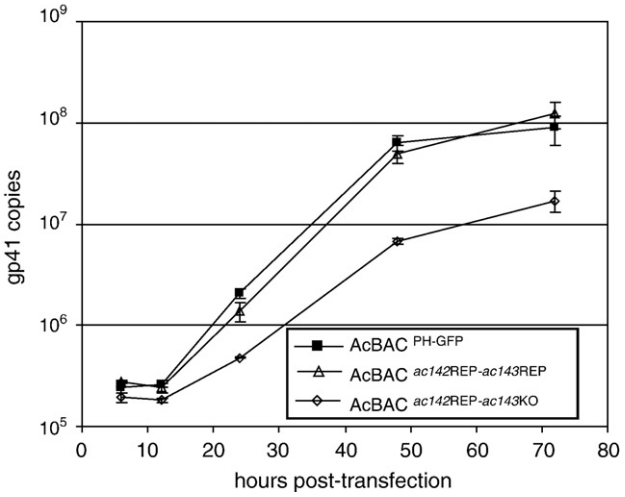

Fig. 4. Quantitative real-time PCR analysis of viral DNA replication. At various hours post-transfection, total DNA was extracted from *Sf*9 cells transfected with AcBAC$^{ac142\text{REP-}ac143\text{KO}}$, AcBAC$^{ac142\text{REP-}ac143\text{REP}}$ and AcBAC$^{\text{PH-GFP}}$, *Dpn*I digested to eliminate input bacmid DNA and analyzed by qPCR as described in Materials and methods. Error bars represent standard deviation.

Light microscopy analysis showed that, at 72 hpt, normal appearing occlusion bodies formed in infected cells with all the constructs (Fig. 2B). Nevertheless, the number of AcBAC$^{ac142\text{REP-}ac143\text{KO}}$-transfected cells which contained occlusion bodies corresponded only to the initially transfected cells (Fig. 2B). In contrast, at 72 hpt, in AcBAC$^{ac142\text{REP-}ac143\text{REP}}$ and AcBAC$^{\text{PH-GFP}}$-transfected cells, almost every cell contained occlusion bodies indicating production of BV and spread of the infection.

Growth curve analysis of AcBAC$^{ac142REP\text{-}ac143KO}$, AcBAC$^{ac142REP\text{-}ac143REP}$ and AcBAC$^{PH\text{-}GFP}$

Our transfection results demonstrated that deletion of *ac143* led to a defect in infectious BV production. Virus growth curve analysis was performed using $TCID_{50}$ (50% tissue culture infective dose) and qPCR to confirm these results and to assess both the effect of deleting *ac143* on virus replication and the replication kinetics of each virus construct. *Sf*9 cells were transfected with each bacmid DNA construct and at selected time-points the BV titers were determined by $TCID_{50}$ end-point dilution. No BV was detectable at any time-point up to 72 hpt in

AcBAC$^{ac142\text{REP-}ac143\text{KO}}$-transfected cells, indicating no infectious virus was produced (Fig. 3A). As expected, *Sf*9 cells transfected with AcBAC$^{ac142\text{REP-}ac143\text{REP}}$ and AcBAC$^{\text{PH-GFP}}$ showed a normal increase in virus production and reached equivalent titers (Fig. 3A). This confirmed that the *ac142-ac143* repair virus was as proficient in virus production as AcBAC$^{\text{PH-GFP}}$ and that the defect in BV production was due to the *ac143* KO and not due to genomic effects at the site of the deletion.

The $TCID_{50}$ end-point dilution assays determine the production of infectious BV but cannot determine if any non-infectious

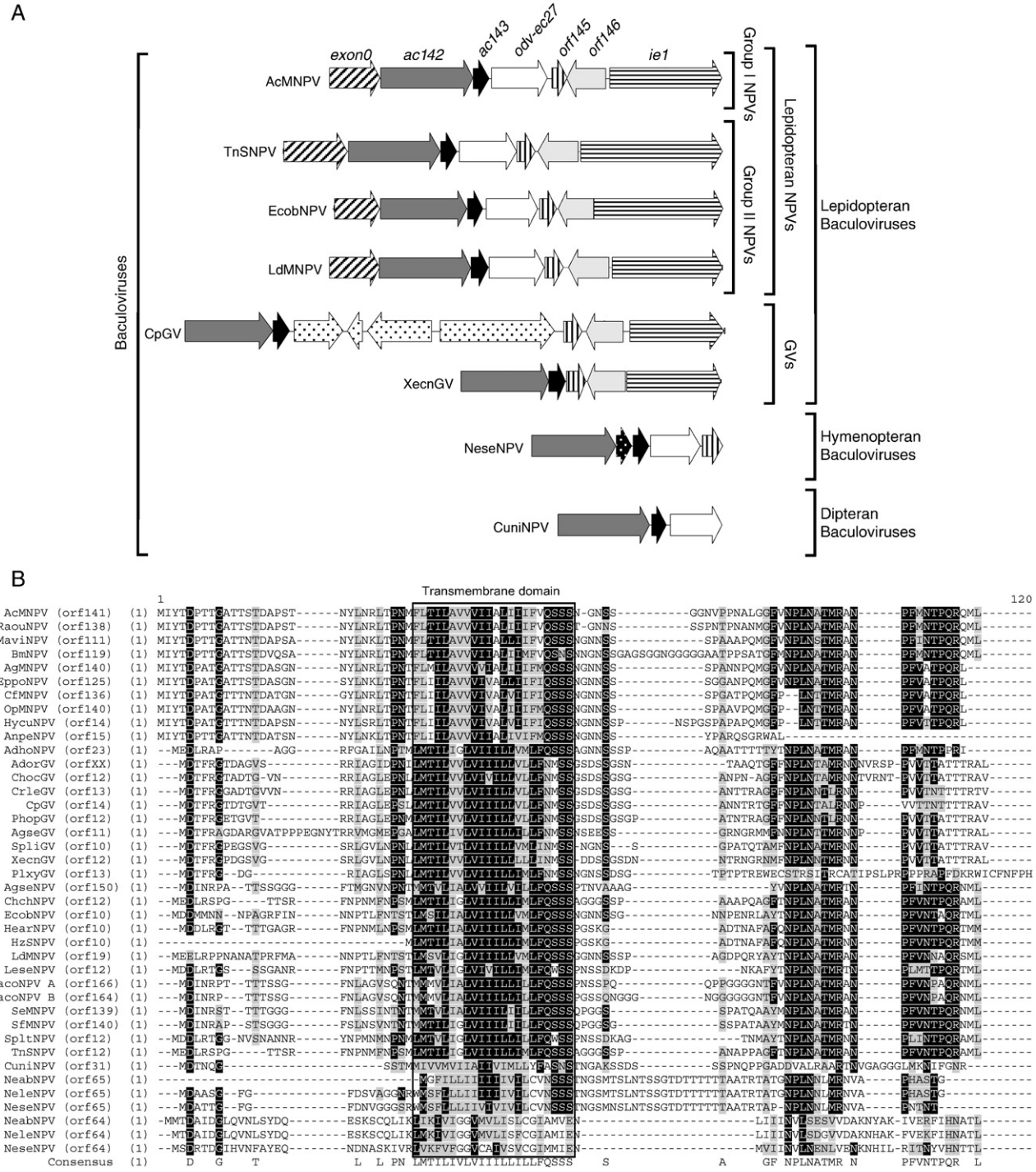

Fig. 5. Orientation of *ac142* and *ac143* homologues and their relative position with respect to each other in the different *Baculoviridae* groups and amino acid alignment of *ac143* homologs. (A) Schematic diagram that highlights the *ac142-ac143* gene cluster in the lepidopteran (alpha- and betabaculoviruses (Jehle et al., 2006)), hymenopteran (gammabaculovirus) and dipteran (deltabaculovirus) baculovirus genomes that have been completely sequenced to date. The hymenopteran baculoviruses contain a unique gene that is potentially also related to *ac143* (indicated as a black arrow with white dots) situated between *ac142* and *ac143* homologues. (B) ClustalW protein alignment of the predicted sequences of *ac143* homologs and the predicted sequence of the second *Neodiprion* gene shown in A. The predicted transmembrane domain found in all homologs is boxed. Black background with white letters indicates identical or conservative changes. Dark grey and light grey represent strongly similar and weakly similar amino acids, respectively. Alignments were performed using the AlignX package of Vector NTI (Invitrogen, Inc.).

BV are being produced. Therefore, to ascertain if non-infectious BV was being produced the titres of AcBAC$^{ac142\text{REP-}ac143\text{KO}}$ and AcBAC$^{\text{PH-GFP}}$ were analyzed by qPCR, which will detect viral genomes regardless of infectivity. There was detectable background of viral genomes present at all time-points analyzed due to genomic DNA present from the bacmid transfection. As expected for AcBAC$^{ac142\text{REP-}ac143\text{REP}}$ and AcBAC$^{\text{PH-GFP}}$-transfected cells, a steady increase in BV was detected up to 72 hpt (Fig. 3B). In contrast, for AcBAC$^{ac142\text{REP-}ac143\text{KO}}$-transfected cells no increase in BV production was detected above the background at any time-point up to 72 hpt (Fig. 3B). Thus, qPCR assay results did not measure any BV production by the *ac143* KO and were in agreement with the $TCID_{50}$ results.

Deletion of ac143 does not affect viral DNA replication in Sf9 cells

The production of occlusion body like structures in AcBAC$^{ac142\text{REP-}ac143\text{KO}}$-transfected cells (Fig. 2B) suggested DNA replication was occurring. However, to determine if *ac143* impacted viral DNA replication, a quantitative analysis was performed to compare the initiation and levels of viral DNA replication in AcBAC$^{ac142\text{REP-}ac143\text{KO}}$, AcBAC$^{ac142\text{REP-}ac143\text{REP}}$ and AcBAC$^{\text{PH-GFP}}$-transfected cells, over a 72 h time-course. Equal amounts of bacmid-transfected *Sf*9 cells were collected at designated time-points, cell lysates were prepared and the total DNA was extracted and then analyzed by qPCR. For all viruses the onset of viral replication occurred between 12 and 24 hpt (Fig. 4). DNA synthesis began increasing at 12 hpt and continued until 48 hpt for AcBAC$^{\text{PH-GFP}}$ and AcBAC$^{ac142\text{REP-}ac143\text{REP}}$ (Fig. 4). DNA synthesis also started increasing after 12 hpt for AcBAC$^{ac142\text{REP-}ac143\text{KO}}$, but at levels that were approximately one log lower than for AcBAC$^{\text{PH-GFP}}$ and AcBAC$^{ac142\text{REP-}ac143\text{REP}}$, correlating with DNA replication being limited to the initially transfected cells (Fig. 4). These results indicated that the onset and level of replication in individual infected cells was unaffected by deletion of *ac143*.

Evolutionary conservation of ac143

Previous analyses have identified 29 core genes that are common to all baculovirus genomes sequenced to date (Garcia-Maruniak et al., 2004; Herniou et al., 2003). The list of core genes included *ac142*, but did not include *ac143*, which was found in lepidopteran and sawfly baculoviruses (proposed alpha-, beta-, and deltabaculoviruses (Jehle et al., 2006)) but not in the dipteran baculoviruses (proposed gammabaculoviruses). The *ac143* promoter is located within the C-terminal region of the *ac142* ORF (Fig. 1) and this linked relationship which has been maintained in all baculovirus groups, is schematically shown in Fig. 5A. The schematic shows that all baculoviruses have retained homologs of *ac142*and *ac143* and that both genes are typically found paired in a gene cluster. In all lepidopteran baculoviruses *ac142-ac143* are found upstream of *ie1*. Within group I and II NPVs the gene organization is consistent across the two groups. However, within granuloviruses there is a variation. For example, CpGV contains an insertion of four ORFs between the homologues of *ac143*and *ac145*. In *Neodiprion* genomes it appears that the *ac142 and ac143* homologous gene clusters are separated by a small ORF. Analysis of this unknown ORF reveals that it is weakly homologous to *ac143* but retains the distinctive hydropathic profile of *ac143*, which includes a predicted transmembrane domain (Fig. 5B). Thus, *Neodiprion* baculoviruses may possess a tandem repeat of *ac143* clustered with an *ac142* homolog. Finally, careful analysis of the dipteran baculovirus CuniNPV revealed a gene cluster containing homologs of *ac142*, *ac144* and a previously unidentified homolog of *ac143*. The presence of this highly conserved gene cluster, the identification of the CuniNPV *ac143* homolog and the results of our present study, provide compelling evidence that *ac143* represents a new baculovirus core gene.

The clustering of *ac142* and *ac143* results in the *ac143* promoter being incorporated and retained within the *ac142* ORF. Previous transcriptional mapping of *ac143* by Braunagel et al. (1996) identified three late transcription start sites (DTAAG). Alignment of the *ac143* promoter with other baculoviruses indicates that all three DTAAG motifs are conserved within the Group I NPVs (alphabaculoviruses) but that two of these motifs are not conserved within Group II NPVs (alphabaculoviruses) (Fig. 6). The DTAAG motif closest to *ac143* translation start site (1 TAAG, Fig. 6) and surrounding sequences are, however, highly conserved within all the NPVs. Granuloviruses, dipteran and hymenopteran baculoviruses retain the promoter within the ORF of the *ac142* homologs, but do not conserve the location of the DTAAGs. Additionally, GVs retain three DTAAG transcriptional start sites, but their relative locations, relative to the *ac143* homolog, differ from those in the NPVs.

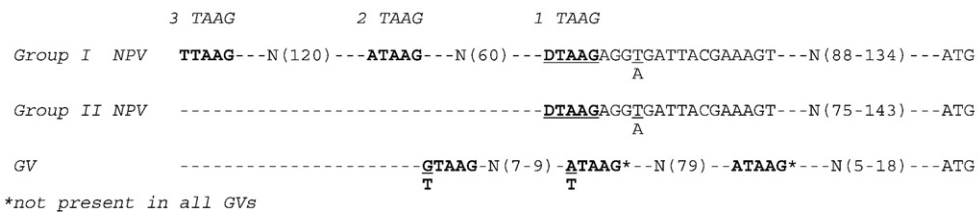

Fig. 6. Location of late promoter motifs in the *ac143* promoter of Group I and II NPVs (alphabaculovirus) and GVs (betabaculovirus). Summary of the location of the DTAAG motifs of the *ac143* promoter based on the 500 bp upstream and including the translation initiation codon in Group I and II NPVs. The position and relative conservation of the first, second and third late promoter motifs, 1 DTAAG, 2 DTAAG and 3 DTAAG, respectively, are shown. The 1 DTAAG NPV sequence shown also includes the highly conserved 16 bp situated downstream. The promoters of the GV *ac143* homologs retain three late promoter motifs but they are in different relative positions to the NPVs and do not align significantly with the NPV promoters.

Due to the strict conservation of the three *ac143* late promoter motifs in group I NPVs, we further analyzed the functionality of this structurally complex promoter by generating four different *ac142* KOs and determining the effect on *ac143* expression and the viral life cycle (Fig. 7). The *ac142* KOs leave either one (AcBac$^{ac142\text{KO-}ac143(1\ \text{TAAG})}$), two (AcBac$^{ac142\text{KO-}ac143(2\ \text{TAAG})}$) or three (AcBac$^{ac142\text{KO-}ac143(3\ \text{TAAG})}$) of the *ac143* late promoter DTAAG motifs intact. A fourth virus was also constructed that left the three DTAAG motifs plus 612 bp upstream of the third DTAAG (AcBAC$^{ac142\text{KO-}ac143(3\ \text{TAAG+ UP})}$) (Fig. 7). The *ac142* KO bacmids were repaired at the *polyhedrin* locus with *ac142*, *polyhedrin* and *gfp* by transposition (Fig. 7). The resulting

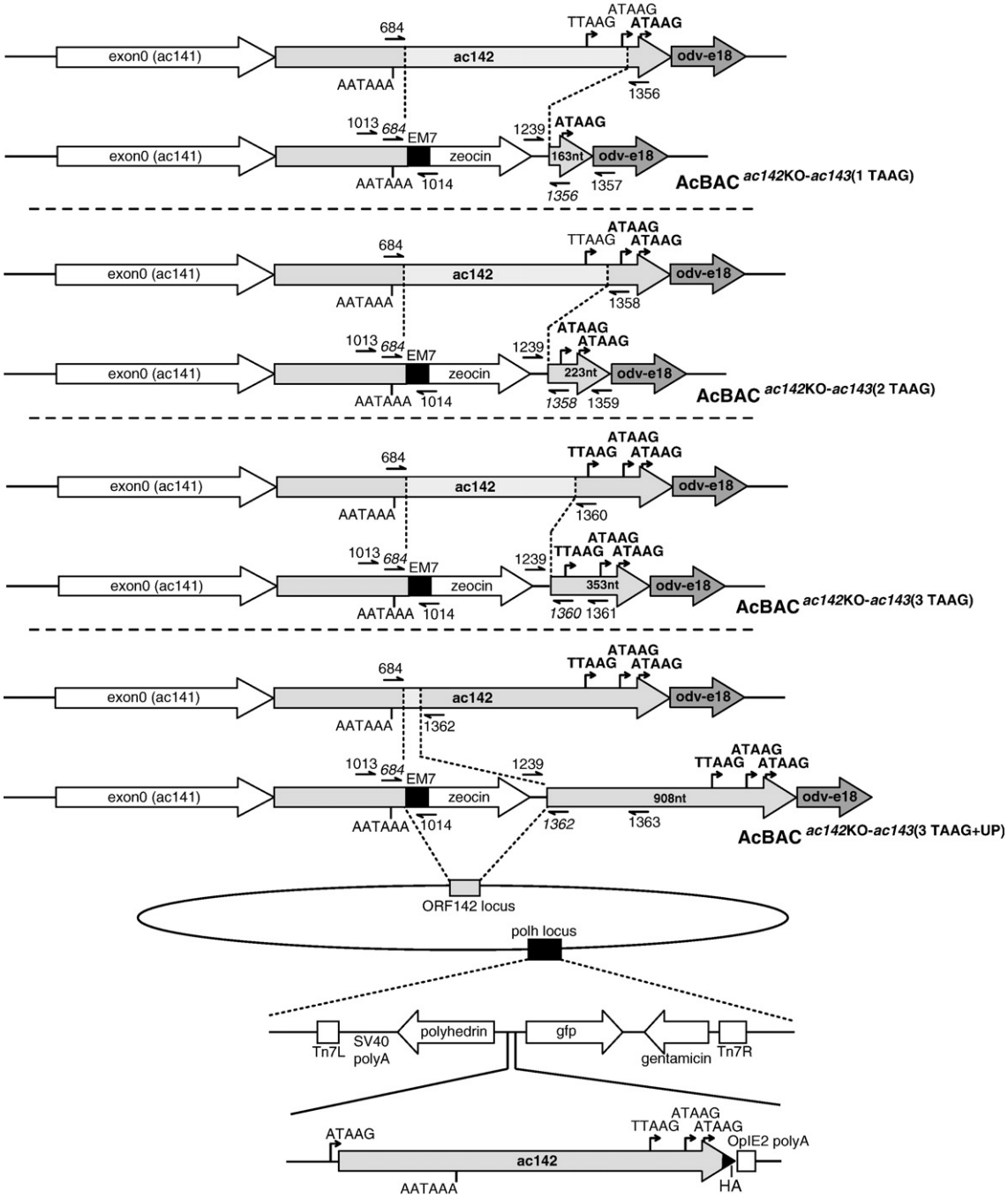

Fig. 7. Construction of *ac142* knockouts and repair AcMNPV bacmids. Schematic diagram describing the construction of AcBAC$^{ac142\text{KO-}ac143(1\ \text{TAAG})}$, AcBAC$^{ac142\text{KO-}ac143(2\ \text{TAAG})}$, AcBAC$^{ac142\text{KO-}ac143(3\ \text{TAAG})}$ and AcBAC$^{ac142\text{KO-}ac143(3\ \text{TAAG+UP})}$. In each case, the *ac142* ORF was partially deleted by replacement with an EM7-*zeocin* gene resistance cassette. In each case the deletion did not affect the polyA signal for *exon0* (*ac141*) included in the *ac142* coding region. Different regions of the *ac143* promoter were left intact in each KO (1 TAAG, 2 TAAG, 3 TAAG or 3 TAAG+UP). The different deletions in the *ac142* locus were confirmed using the indicated primer pairs. The number of nucleotides left intact of the *ac143* promoter from the start codon (ATG) are indicated along with the relative locations of the DTAAG motifs. The *ac142* ORF which was inserted at the *polyhedrin* locus to rescue the *ac142* deletion is driven by its own promoter and includes an in-frame C-terminal HA-epitope.

ac142 KO bacmids, were examined by PCR to confirm the correct insertion of the *zeocin* gene cassette into the *ac142* locus (data not shown).

Viral replication in Sf9 cells transfected with ac143 promoter deletions

To determine if the different deletions in the *ac143* promoter region caused any effect on viral replication, *Sf*9 cells were transfected with AcBAC$^{ac142\text{REP-}ac143(1\ TAAG)}$, AcBAC$^{ac142\text{REP-}ac143(2\ TAAG)}$, AcBAC$^{ac142\text{REP-}ac143(3\ TAAG)}$, AcBAC$^{ac142\text{REP-}ac143(3\ TAAG+UP)}$ and AcBAC$^{PH\text{-}GFP}$ and were monitored by fluorescence microscopy. No difference was observed among the viruses at 24 hpt, indicating comparable transfection efficiencies (Fig. 8A). At 48 hpt, fluorescence was observed in almost all AcBAC$^{PH\text{-}GFP}$-transfected cells (Fig. 8A), indicating the spread of viral infection. In contrast, at 48 hpt, in cells transfected with the *ac143* promoter deletion bacmids an increase in the levels of fluorescence was observed, but the levels were consistently lower than for AcBAC$^{PH\text{-}GFP}$. This suggested that *ac143* promoter deletion viruses were capable of generating infectious BV from the initial transfection but not as proficiently as AcBAC$^{PH\text{-}GFP}$. A progression in the levels of fluorescence was observed (Fig. 8A). Based on fluorescence, by 72 hpt the greatest number of infected cells was observed in cells transfected with AcBAC$^{ac142\text{REP-}ac143(3\ TAAG)}$, followed by AcBAC$^{ac142\text{REP-}ac143(3\ TAAG+UP)}$, AcBAC$^{ac142\text{REP-}ac143(2\ TAAG)}$ and AcBAC$^{ac142\text{REP-}ac143(1\ TAAG)}$, which produced the lowest levels. At 72 hpt fluorescence was observed in almost all AcBAC$^{PH\text{-}GFP}$-transfected cells (Fig. 8A). By 120 hpt all cells transfected by any of the viruses were infected and the majority exhibited the formation of polyhedra (Fig. 8C).

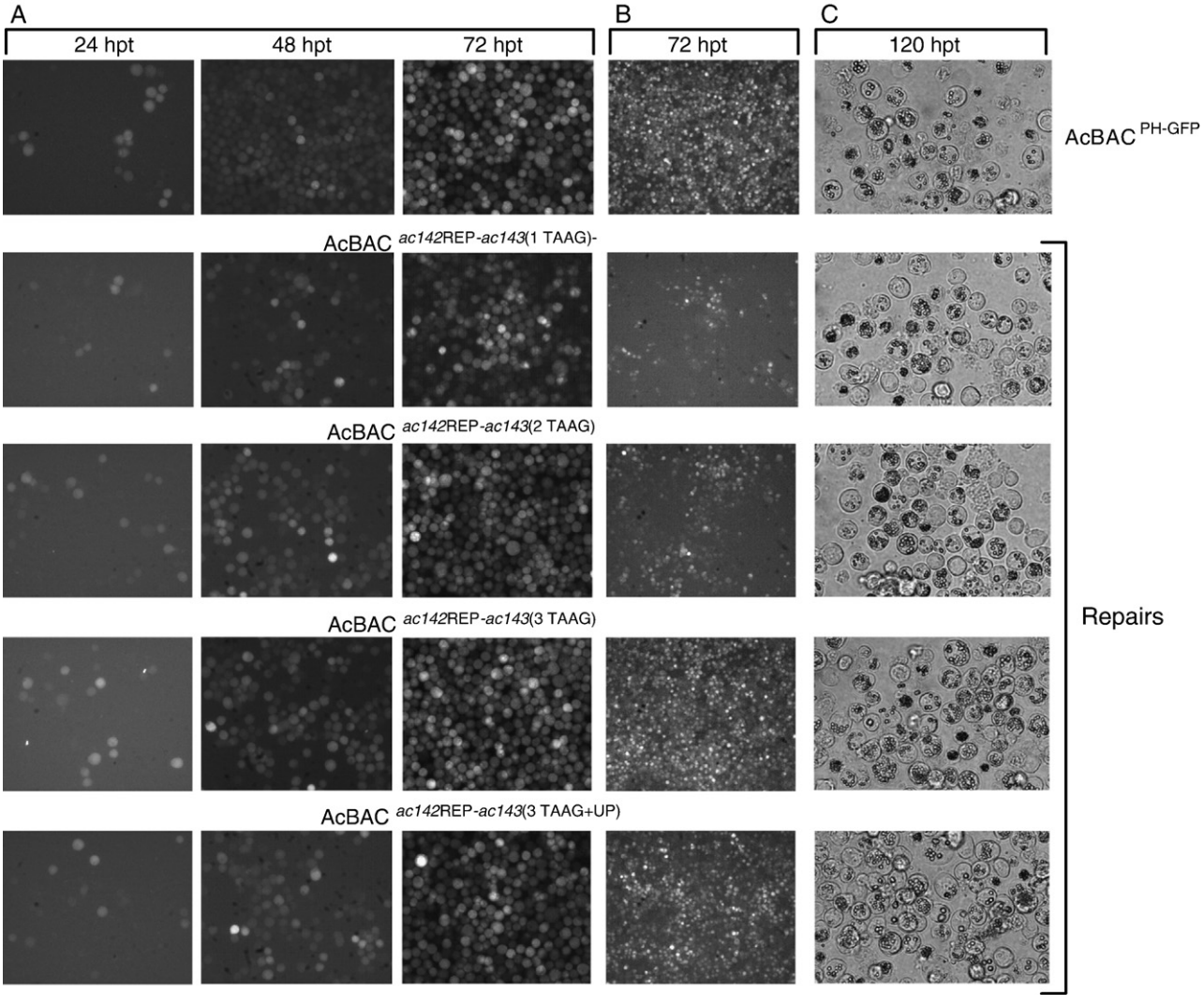

Fig. 8. Viral replication analysis of *ac143* promoter deletions transfected into *Sf*9 cells. (A) Fluorescence microscopy showing the progression of the infection in *Sf*9 cells transfected with AcBAC$^{ac142\text{REP-}ac143(1\ TAAG)}$, AcBAC$^{ac142\text{REP-}ac143(2\ TAAG)}$, AcBAC$^{ac142\text{REP-}ac143(3\ TAAG)}$, AcBAC$^{ac142\text{REP-}ac143(3\ TAAG+UP)}$ and AcBAC$^{PH\text{-}GFP}$ at 24, 48 and 72 hpt. (B) Fluorescence microscopy at 72 hpt showing transfected *Sf*9 cells overlaid with agarose to restrict BV movement to adjoining cells to monitor the difference in the progression of the infection between the different deletion constructs and AcBAC$^{PH\text{-}GFP}$. (C) Light microscopy of *Sf*9 cells transfected with AcBAC$^{ac142\text{REP-}ac143(1\ TAAG)}$, AcBAC$^{ac142\text{REP-}ac143(2\ TAAG)}$, AcBAC$^{ac142\text{REP-}ac143(3\ TAAG)}$, AcBAC$^{ac142\text{REP-}ac143(3\ TAAG+UP)}$ and AcBAC$^{PH\text{-}GFP}$ at 120 hpt. Most of the cells transfected with the repair constructs developed approximately equal levels of normal appearing occlusion bodies.

To further compare the spread of virus between AcBAC$^{PH\text{-}GFP}$ and the *ac142* repairs, transfected cells were overlaid with agarose to restrict movement of BV to adjoining cells. Under these conditions, by 72 hpt the same differential progression in viral infection was observed for the repairs compared to AcBAC$^{PH\text{-}GFP}$ (Fig. 8B).

Growth curve analysis of ac143 promoter deletions

The fluorescence microscopy results showed that the deletion of different regions of the *ac143* promoter affected viral replication to varying degrees. To further assess the effect of the *ac143* promoter deletions on virus replication, BV growth curves were analyzed by qPCR. *Sf*9 cells were transfected with the different bacmid DNA repair constructs and, at selected time-points, the BV titers were determined. As mentioned previously, due to the nature of bacmid transfection there is a detectable background of viral genomes present at all time-points analyzed. All viruses exhibited a steady increase in BV up to 72 hpt and, at this time-point, there was no significant difference in BV levels (Fig. 9). However, at 24, 36 and 48 hpt BV levels were significantly lower for all the *ac142* repairs compared to AcBAC$^{PH\text{-}GFP}$. The lowest levels corresponded to AcBAC$^{ac142\text{REP-}ac143(1\ TAAG)}$, followed by AcBAC$^{ac142\text{REP-}ac143(3\ TAAG+UP)}$ and lastly AcBAC$^{ac142\text{REP-}ac143(2\ TAAG)}$ and AcBAC$^{ac142\text{REP-}ac143(3\ TAAG)}$, both of which presented very similar dynamics. The qPCR results therefore confirmed that BV production was less efficient in all the *ac142* repairs compared to AcBAC$^{PH\text{-}GFP}$, but that AcBAC$^{PH\text{-}GFP}$ (wild-type) levels were attained at late times post-

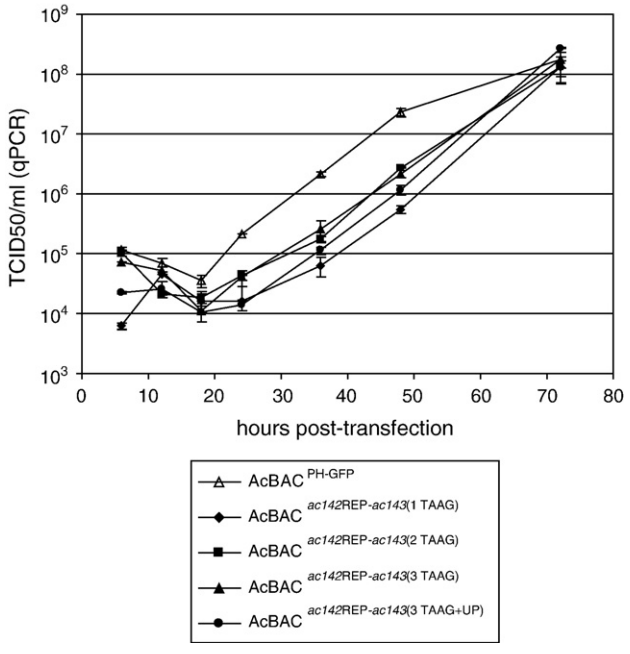

Fig. 9. Virus growth curve of *Sf*9 cells transfected with *ac143* promoter deletion bacmids and AcBAC$^{PH\text{-}GFP}$. To determine the effect of *ac143* promoter deletions on BV production *Sf*9 cells were transfected with AcBAC$^{ac142\text{REP-}ac143(1\ TAAG)}$, AcBAC$^{ac142\text{REP-}ac143(2\ TAAG)}$, AcBAC$^{ac142\text{REP-}ac143(3\ TAAG)}$, AcBAC$^{ac142\text{REP-}ac143(3\ TAAG+UP)}$ and AcBAC$^{PH\text{-}GFP}$. Viral titers were determined at the designated time-points by qPCR analysis.

transfection. This was in agreement with results obtained through fluorescence microscopy and agarose overlay.

Transcriptional analysis of Sf9 cells transfected with ac143 promoter deletion bacmids

A schematic diagram of the *ac143* specific transcripts is shown in Fig. 10A. Previous Northern blot analyses of cells infected with AcMNPV, determined that the *ac143* transcripts are 1.5 and 2 kb in size and that they were detectable from 16 h post-infection (hpi) with maximal steady-state levels around 36 hpi and high levels at 72 hpi (Braunagel et al., 1996).

To determine if the deletion of different regions of the *ac143* promoter impacted viral transcription, a Northern blot analysis of AcBAC$^{ac142\text{REP-}ac143\text{KO}}$, AcBAC$^{ac142\text{REP-}ac143(1\ TAAG)}$, AcBAC$^{ac142\text{REP-}ac143(2\ TAAG)}$, AcBAC$^{ac142\text{REP-}ac143(3\ TAAG)}$, AcBAC$^{ac142\text{REP-}ac143(3\ TAAG+UP)}$ and AcBAC$^{PH\text{-}GFP}$-transfected cells was performed using a strand specific probe homologous to the *ac143* coding region (Fig. 10A). For AcBAC$^{PH\text{-}GFP}$-transfected cells, three *ac143* RNA bands (1.0, 1.3 and 2.3 kb in size) were detected from 24 to 72 hpt (Fig. 10B). These sizes were in approximate agreement with transcription initiating at the *ac143* late promoter motifs (TTAAG, ATAAG and ATAAG) and their termination at the first, second and third polyA signal sequences (AATAAA) downstream of the coding region (included within *ac144* (*odv-ec27*) and *ac146*) (Fig. 10A). Transcription initiation from DTAAG 2 or 3 would result in *ac143* mRNAs that are 65 or 189 nt larger relative to transcripts from the first DTAAG motif. The disparity in size between the 1.5 and 2 kb bands found by Braunagel et al. (1996) and the 1.3 and 2.3 kb bands identified in this study, probably stem from the percentage gel used to resolve the RNA species on the Northern blot. In this study we also detected a 1.0 kb band that was probably not resolved from the 1.3 kb band observed in the previous analysis of *ac143*. For all the constructs, the *ac143* specific 1.3 kb RNA was the major transcript expressed. Similar to AcBAC$^{PH\text{-}GFP}$-transfected cells, all transcripts were detected after the onset of DNA replication and increased in steady-state levels from 24 to 72 hpt.

Significantly different expression patterns for each of the three transcripts were observed between AcBAC$^{PH\text{-}GFP}$ and the different repair constructs (Fig. 10B). The expression levels of each transcript at each time-point was determined and graphically compared for each virus (Figs. 10C, D, and E). For AcBAC$^{PH\text{-}GFP}$, the steady-state levels of all transcripts were maximal by 48 hpt and decreased at 72 hpt. In contrast, for all the repair constructs, the steady-state levels of the transcripts increased up to 72 hpt and reached maximal levels at 72 hpt (Figs. 10C, D, and E).

AcBAC$^{ac142\text{REP-}ac143(1\ TAAG)}$ which deletes both DTAAG 2 and 3, appeared to be the most transcriptionally delayed virus. The 1.0 kb and 1.3 kb bands were first detectable at 48 hpt and the 2.3 kb mRNA was not detectable at any time-point. In AcBAC$^{ac142\text{REP-}ac143(2\ TAAG)}$ transfected cells the 1.0 kb transcript was detected later than for AcBAC$^{PH\text{-}GFP}$ but surprisingly the levels became higher at 48 and 72 hpt. The 1.3 kb primary transcript was detected at approximately the same time

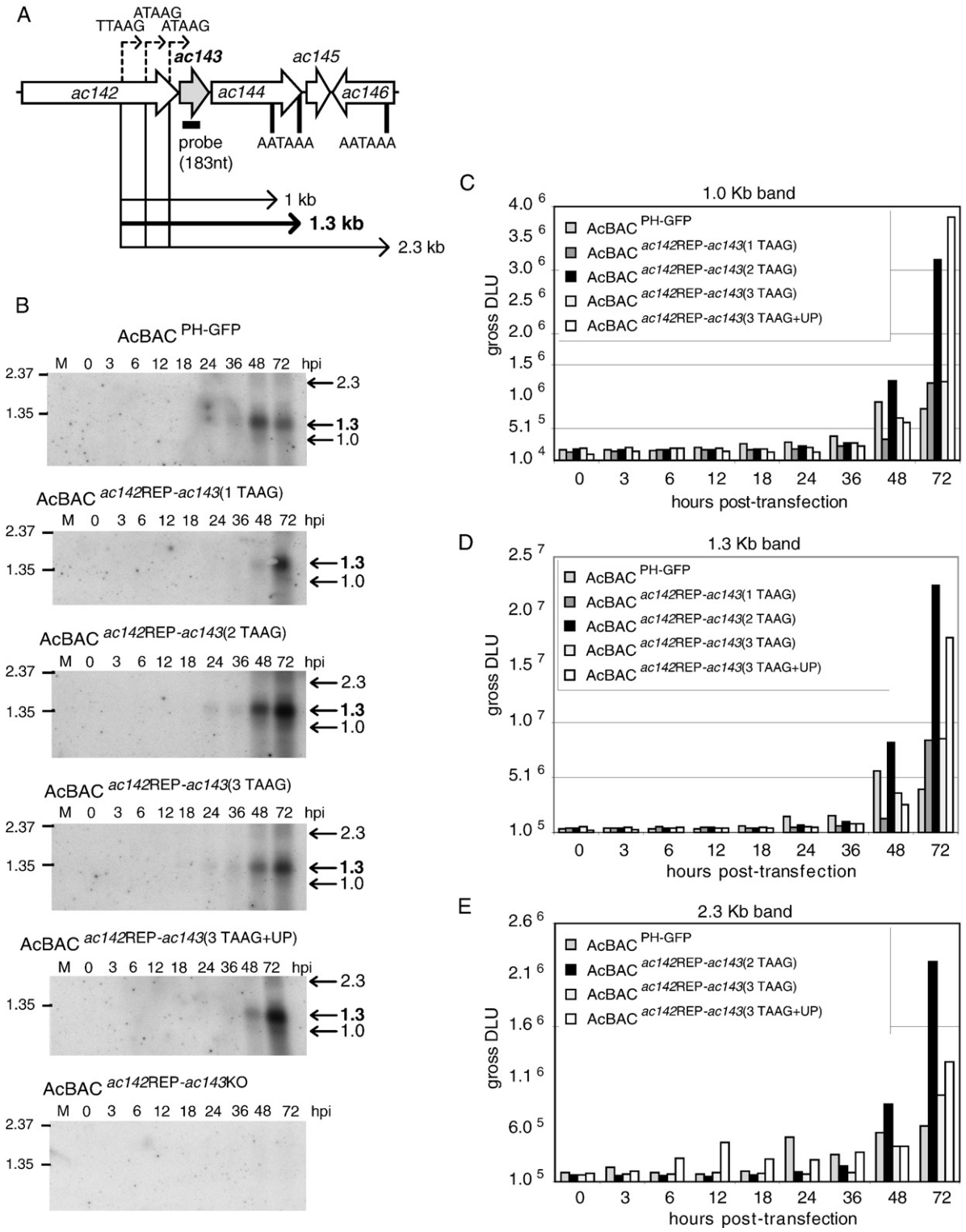

Fig. 10. Comparative Northern blot analysis of *ac143* transcription in *Sf*9 cells transfected with *ac143* promoter deletion bacmids and AcBAC$^{PH\text{-}GFP}$. (A) Schematic map showing the relative sizes, positions and orientations of the *ac142*, *ac143*, *ac144* (*odv-ec27*), *ac145* and *ac146* ORFs. The *ac143* specific transcripts (Braunagel et al., 1996) detectable by the single-stranded probe homologous to *ac143* (indicated as a black line) are shown below the ORFs. Sizes are based on the location of late transcription start sites and polyadenylation signals. The 1.3 kb RNA (bold) was the major transcript detected. (B) Northern blot analysis of *ac143* transcription in *Sf*9 cells transfected with either AcBAC$^{PH\text{-}GFP}$, AcBAC$^{ac142\text{REP-}ac143(1\ TAAG)}$, AcBAC$^{ac142\text{REP-}ac143(2\ TAAG)}$, AcBAC$^{ac142\text{REP-}ac143(3\ TAAG)}$, AcBAC$^{ac142\text{REP-}ac143(3\ TAAG+UP)}$ or AcBAC$^{ac142\text{REP-}ac143\text{KO}}$ from 0 to 72 hpt. The identified RNA bands and their sizes (kb) are indicated on the right of the photograph. Size markers are shown on the left (kb). (C–E) Graphs showing the relative level and time of expression of the *ac143* 1.0, 1.3 and 2.3 kb mRNAs from 0 to 72 hpt. The mRNAs were quantified using a phosphorimager. DLU, digital light units.

but reached much higher levels at 48 and 72 hpt. This would suggest that the deleted upstream sequences, which include the third DTAAG, are required for down regulating the 1.3 kb mRNA expression. This was in agreement with the expression of the 1.3 kb band from AcBAC$^{ac142\text{REP-}ac143(3\ \text{TAAG})}$ transfected cells, which was lower and more similar to AcBAC$^{\text{PH-GFP}}$ by 48 and 72 hpt. Surprisingly however, AcBAC$^{ac142\text{REP-}ac143(3\ \text{TAAG+UP})}$, which retains the over 900 nt of upstream sequences including the 3 DTAAGs, has significantly different expression compared to AcBAC$^{\text{PH-GFP}}$. The 1.0 kb transcript was detected only by 72 hpt and at higher levels than AcBAC$^{\text{PH-GFP}}$. The 1.3 kb transcript was detected at 48 and 72 hpt and also reached higher levels than AcBAC$^{\text{PH-GFP}}$.

These results showed that any deletion of the *ac143* upstream sequences within the *ac142* ORF affected *ac143* expression and viral replication. This data supports the hypothesis that a conservation of the *ac142-ac143* gene cluster is necessary to maintain the transcriptional fidelity of both genes.

Discussion

AcMNPV *ac143* (*odv-e18*) has previously been shown to be a late gene that encodes a structural protein of the ODV located in the virion envelope. It is also detected in viral induced intranuclear microvesicles and membranes formed prior to nucleocapsid envelopment (Braunagel et al., 1996). In this study we have further examined the role of AcMNPV *ac143* in viral replication and determined that it is an essential gene in the viral life cycle and, in addition, that it is a baculovirus core gene. Using the AcMNPV bacmid system (Luckow et al., 1993), an *ac143* KO virus (AcBAC$^{ac142\text{REP-}ac143\text{KO}}$) was used to demonstrate that *ac143* is essential for BV production and that viral infection is restricted to a single cell. Additionally, we analyzed the effect on viral replication of deleting various portions of the highly conserved *ac143* promoter region which is located within the ORF of the baculovirus core gene *ac142*. Our results showed that any perturbation of the *ac143* promoter region resulted in a subsequent reduction in initial BV production, but that levels would recover to those of AcBAC$^{\text{PH-GFP}}$ at late times post-infection.

Previous sequence analyses of the dipteran baculovirus, CuniNPV, had suggested that it lacks an *ac143* homologue (Afonso et al., 2001; Garcia-Maruniak et al., 2004). However, our analysis of the CuniNPV genome identified a gene that is contiguous and clustered with the *ac142* homologue, is found in the same orientation and is similar in size to *ac143* (Fig. 5). The predicted protein of the CuniNPV ORF, *cuni31*, shows homology and retains the distinct transmembrane domain structure of all the *ac143* homologs (Fig. 5B). The presence of an *ac143* homolog in CuniNPV would therefore make it a baculovirus core gene. This brings the total number of core genes to 30 and not 29, as previously reported (Garcia-Maruniak et al., 2004).

Apart from being core genes, *ac142* and *ac143* also form a gene cluster, which is a significant finding as gene order is generally poorly conserved among baculoviruses. Only one other conserved cluster of genes has been described to date and includes the four core genes *helicase*, *lef5*, *ac96* and *38K* (Herniou et al., 2003; Wu et al., 2006). The evolutionary conservation of the *ac143-ac143* gene cluster would predict a functional necessity for their association. This conclusion correlates with the deletions in the *ac143* promoter region which showed that any insertion in that region affected BV production. Indeed, the only repair virus that rescued normal BV production was AcBAC$^{ac142\text{REP-}ac143\text{REP}}$ (Fig. 1). In this case *ac142* and *ac143* were repaired as a unit and the virus showed no significant difference with AcBAC$^{\text{PH-GFP}}$ in viral replication, BV titer or DNA replication (Figs. 2, 3, and 4). Interestingly, the gene cluster in the hymenopteran baculoviruses contains a unique second ORF that is predicted to code for an additional *ac143*-like protein that retains the transmembrane domain in the N-half of the protein (Fig. 5) (Duffy et al., 2006; Garcia-Maruniak et al., 2004; Lauzon et al., 2006, 2004). Thus, it is possible that this second hymenopteran ORF may have a function either auxiliary to, or complementary to *ac143*.

Ac143 transcripts have been shown to initiate from the three upstream DTAAG sequences included in the *ac142* coding region (Braunagel et al., 1996) and that the DTAAG sequence closest to the *ac143* initiation codon (Fig. 6, 1 TAAG) was the most active transcriptional initiation site. To analyze the effect of sequentially deleting sequences upstream containing the two other DTAAG sequences (Fig. 6, 2 and 3 TAAG), four different *ac142* KOs were generated which left either one, two, or three of the DTAAG sequences intact. The Northern blot analyses of these deletion mutants revealed that the temporal transcriptional pattern and the expression levels of *ac143* were variably affected by the different deletions (Fig. 10). These results indicated that all the deletions performed in the *ac143* promoter region affected viral replication causing significant differences in BV production and RNA transcription when compared to AcBAC$^{\text{PH-GFP}}$. AcBAC$^{ac142\text{REP-}ac143(1\ \text{TAAG})}$ demonstrated the most severely impaired viral replication. In general it appeared that the upstream DTAAG sequences (2 and 3 TAAG) enabled earlier detectable expression and down regulated maximum levels of expression. Therefore the upstream promoter sequences containing the two additional transcriptional starts, though non-essential, are required for modulating *ac143* expression.

The 3 DTAAG motifs in the *ac143* promoter are only conserved in Group I NPVs, but the first DTAAG and surrounding sequences are highly conserved in all NPVs (Fig. 6). This conserved sequence includes the DTAAG and 16 nt downstream. A comparison of these downstream sequences with the rest of the AcMNPV genome indicated that similar motifs with 2 or 3 nt differences are found throughout the genome in various promoters including *polyhedrin*, *lef-10*, *gp41*, *ac154* and *gp37* (data not shown). This would suggest that this motif may be a regulatory element required for binding *trans*-acting factors and regulating baculovirus gene expression.

The evolutionary conservation and transcriptional interdependence of *ac142* and *ac143* expression, suggests there may be functional interaction between these two proteins. Deletion of either gene gives the same single cell phenotype and both gene knockout viruses are unable to produce BV (McCarthy et al., 2008; Vanarsdall et al., 2007). In addition, our recent findings have shown that in the absence of a complete *ac142* nucleocapsids cannot acquire nuclear viral envelopes to form

Table 1
Primer pairs used to generate the *ac142* and *ac142-ac143* knockouts

Virus	Primers [a, b]	
All KOs	684 (upper)	GGTTTCTTGTTCGACGATGCGTACGTGGATTGGAATGGTGTGCGAATGTGT
		TTCGGATCTCTGCAGC
AcBAC^{ac142}REP-$ac143$KO	1234 (lower)	TATTAAAGCAATAATTACTACTACAGCCAAGATGGTCAAGAACATGTTTG
		CTTATCTTTTTATCTTTCGAGGTCGACCCCCCTG
AcBAC^{ac142}REP-$ac143$(1 TAAG)	1356 (lower)	ATATGCAGGCACCGTGTTTGAGAACACGTGTTTGACCAAAAAAACTTTTT
		TCGAGGTCGACCCCCCTG
AcBAC^{ac142}REP-$ac143$(2 TAAG)	1358 (lower)	AACAACATACACGTCGCCCGTCAAACGGACCGGCGGCGAACTCTGCCGGT
		TCGAGGTCGACCCCCCTG
AcBAC^{ac142}REP-$ac143$(3 TAAG)	1360 (lower)	TGCTTGGGCGCGTAGAACGCGTTCATAGTGCCTTTCAATTGCAAAAAGTCTCGAGGTCGACCCCCCTG
AcBAC^{ac142}REP-$ac143$(3 TAAG+UP)	1362 (lower)	CCCAGTAGATACAGTCGGAACGGATGCATGTTGTTATCTAATCGCGGCGCTCGAGGTCGACCCCCCTG

[a] Primer sequences are 5′ to 3′.
[b] The underlined sequences are those homologous to the corresponding flanking regions in the bacmid.

ODV. Without an envelope the nucleocapsids are not occluded within the polyhedra and the polyhedra produced are empty of virions. (McCarthy et al., 2008). Interestingly, Braunagel et al. (1996) showed that *ac143* was associated with the viral induced intranuclear membranes and microvesicles prior to nucleocapsid envelopment. The logical prediction from these two findings is that *ac142* (in the nucleocapsid) and *ac143* (in the viral membrane) interact so that nucleocapsids can sequester the viral membrane to form enveloped virions. In support of this, fractionation of BV showed that *ac142* localized principally to the nucleocapsid fraction while a minor fraction was consistently found in the envelope fraction (McCarthy et al., 2008). Further studies need to be performed to determine if *ac143* is also necessary for bundles of nucleocapsids to acquire nuclear envelopes in order to form ODV. Additionally, it will be important to establish if *ac143* is also a BV envelope protein and if it is essential for nucleocapsid formation.

In conclusion, this study has shown that *ac143* is an essential baculovirus gene that clusters with *ac142*. Deletions in the *ac143* promoter region produced viruses with significantly different BV production and RNA transcription patterns when compared to AcBAC$^{PH\text{-}GFP}$. This indicates a tight genomic interdependence between *ac142* and *ac143*. Apart from the *helicase*, *lef5*, *ac96* and *38 K* cluster, the *ac142-ac143* cluster represents the second and only other gene cluster found in all baculoviruses. The identification of the CuniNPV *ac143* homolog indicates that there are 30 core genes common to all baculoviruses sequenced to date.

Materials and methods

Viruses and cells

The AcMNPV bacmid bMON14272 (Invitrogen Life Technologies) was derived from the AcMNPV strain E2 and maintained in DH10B cells as described previously (Luckow et al., 1993). *Sf*9 (*Spodoptera frugiperda* IPLB-*Sf*21-AE clonal isolate 9) insect cells were cultured in suspension at 27 °C in TC100 medium supplemented with 10% fetal bovine serum.

Construction of ac142-ac143 and ac142 knockout AcMNPV bacmids

An AcMNPV bacmid (bMON14272) was used to generate the *ac142-ac143* and *ac142* KO viruses by recombination in *Escherichia coli*, as previously described (Hou et al., 2002; Lin and Blissard, 2002; Lung et al., 2003; Stewart et al., 2005). A *zeocin* resistance cassette was amplified using different primer pairs for the different KO bacmids using p2ZeoKS as template (Table 1; Figs. 1 and 7). The *zeocin* cassette PCR fragments were gel purified and electroporated into *E. coli* BW25113-pKD46 cells, which contained the AcMNPV bacmid bMON14272. The electroporated cells were incubated at 37 °C for 2 h in 1 ml of LB medium and plated onto agar medium containing 30 μg/ml of zeocin and 50 μg/ml of kanamycin. Plates were incubated at 37 °C overnight and colonies resistant to both zeocin and kanamycin were selected and further confirmed by PCR.

Table 2
Primer pairs used to confirm the correct insertion of the *zeocin* gene cassette in the upstream (5′) and downstream (3′) regions of the different KO bacmids

Region	Virus	Primers [a]	
5′	All KOs	1013 (upper)	GATGATGGCTTTCCTGTACGCTGAA
		1014 (lower)	CCGATATACTATGCCGATGATT
3′	All KOs	1239 (upper)	CTGACCGACGCCGACCAA
	AcBAC^{ac142}KO-$ac143$(1 TAAG)	1357 (lower)	GCTAGTCGTAGCGCCAGT
	AcBAC^{ac142}KO-$ac143$(2 TAAG)	1359 (lower)	CCGAGTCGGGGATTAATA
	AcBAC^{ac142}KO-$ac143$(3 TAAG)	1361 (lower)	AACTCTGCCGGTACACGA
	AcBAC^{ac142}KO-$ac143$(3 TAAG+UP)	1363 (lower)	ACTGGGCGTCGAATATGT

[a] Primer sequences are 5′ to 3′.

Different primer pairs were used to confirm the correct insertion of the *zeocin* gene cassette in the upstream and downstream regions of the AcMNPV bacmid genomes (Table 2; Figs. 1 and 7). One recombinant bacmid with the correct PCR confirmations was selected for each KO. The resulting *ac142-ac143* KO bacmid, was named AcBAC$^{ac142\text{KO-}ac143\text{KO-PH-}}$ (Figs. 1 and 7). To generate bacmids containing the *polyhedrin* and *gfp* genes, the transfer vector pFAcT-GFP was used as previously described (Dai et al., 2004). To generate an *ac142-ac143* KO bacmid repaired with *ac142* and *ac143*, the repair transfer vector pFAcT-GFP-OpIE2pA-*ac142-ac143* was constructed as follows. Primers 1019 (5′-GCC*CTGCA-G*ACGGCCACCACGCACGCAAA-3′) and 1501 (5′-TCA*CCCGGG*CTACAACATTTGCCTTTGAGG-3′), which contain *Pst*I and *Xma*I sites (underlined sequences), respectively, were used to amplify ORFs *ac142* and *ac143* with their native promoters. The digested PCR fragment was sub-cloned into pBS+. Subsequently the *ac142-ac143* fragment was digested with *Pst*I and *Xma*I, gel purified and ligated into pFAcT-GFP-OpIE2pA (McCarthy et al., 2008) digested with the same enzymes. The resulting repair transfer vector, pFAcT-GFP-*ac142-ac143*, was used to generate AcBAC$^{ac142\text{REP-}ac143\text{REP}}$.

To generate *ac142-ac143* and *ac142* KO bacmids repaired with an HA-tagged version of *ac142*, the repair transfer vector pFAcT-GFP-*ac142* HA was constructed as previously described (McCarthy et al., 2008) and used to generate AcBAC$^{ac142\text{REP-}ac143\text{KO}}$, AcBAC$^{ac142\text{REP-}ac143(1\ \text{TAAG})}$, AcBAC$^{ac142\text{REP-}ac143(2\ \text{TAAG})}$, AcBAC$^{ac142\text{REP-}ac143(3\ \text{TAAG})}$ and AcBAC$^{ac142\text{REP-}ac143(3\ \text{TAAG+UP})}$.

Repair sequences were inserted into the *polyhedrin* locus of the AcMNPV bacmid by Tn7-mediated transposition as previously described (Luckow et al., 1993). Briefly, electro-competent DH10B *E. coli* cells containing helper plasmid pMON7124 and bacmid DNA, were transformed with the transfer vectors described above. Following a 5 h incubation at 37 °C in 1 ml LB, cells were plated onto agar medium containing 50 μg/ml kanamycin, 7 μg/ml gentamicin, 10 μg/ml tetracycline, 30 μg/ml zeocin, 100 μg/ml X-Gal and 40 μg/ml IPTG. Plates were then incubated at 37 °C for 24 h and white colonies were selected and streaked to fresh plates. The correct phenotype was then confirmed by PCR. Transposition events were confirmed by GFP expression and occlusion body formation in bacmid DNA-transfected *Sf*9 cells.

Time course analysis and titration of BV production

*Sf*9 cells (1.0×10^6 cells/35 mm-diameter well of a six-well plate) were transfected as previously described (Stewart et al., 2005) with 1.0 μg of each bacmid construct (AcBAC$^{ac142\text{REP-}ac143\text{KO}}$, AcBAC$^{ac142\text{REP-}ac143\text{REP}}$ or AcBAC$^{\text{PH-GFP}}$). At various hpt, the supernatant containing the BV was harvested and cell debris was removed by centrifugation (6000 ×*g* for 3 min). BV production was determined in duplicate by end-point dilution using *Sf*9 cells in a 96-well microtiter plate format. Titres were also determined by quantitative polymerase chain reaction (qPCR) as previously described (Lo and Chao, 2004). Primers 850 (5′-TTTGGCAAGGGAACTTTGTC-3′) and 851 (5′-ACAAACCTGGCAGGAGAGAG-3′) amplify a 100 bp genomic fragment of *ac126* (*chitinase*). A stock of wild-type AcMNPV (2.5×10^8 pfu/mL), previously titered by end-point dilution, was used as a standard. Supernatants containing BV were harvested and cell debris was removed by centrifugation (8000 ×*g* for 5 min). An aliquot of each of these supernatants (100 μl) was processed using the Roche High Pure Viral Nucleic Acid Kit (Cat. No. 11858874001).

An aliquot of each purified DNA sample (8 μl) was combined with the New England Biolabs SYBR Master Mix (DyNAmo HS SYBR Green qPCR Kit, Cat. No. F410-L) and the qPCR primers in a 20 μl reaction. The samples were analyzed in a Stratagene MX4000 qPCR cycler under the following conditions: 1 cycle of 95 °C for 15 min; 40 cycles of 95 °C for 30 s, 52 °C for 24 s, 72 °C for 30 s; 1 cycle of 95 °C for 1 min; 41 cycles of 55 °C for 30 s. The results were analyzed using Stratagene MX4000 software.

Plaque assay

*Sf*9 cells (1.0×10^6 cells/35 mm-diameter well of a six-well plate) were transfected with 1.0 μg of each bacmid construct (AcBAC$^{ac142\text{REP-}ac143(1\ \text{TAAG})}$, AcBAC$^{ac142\text{REP-}ac143(2\ \text{TAAG})}$, AcBAC$^{ac142\text{REP-}ac143(3\ \text{TAAG})}$, AcBAC$^{ac142\text{REP-}ac143(3\ \text{TAAG+UP})}$ or AcBAC$^{\text{PH-GFP}}$). After a 3 h incubation period, the transfection supernatant was removed and the cells were washed with 1 ml of Grace's medium. Cells were overlaid with 2 ml of TC100 medium containing 1.5% low-melting-point agarose (SeaPlaque) pre-equilibrated to 37 °C, followed by incubation at 27 °C in a humid box for 4 days. The cells were observed by fluorescence and light microscopy from 48 hpt onward.

DNA replication using quantitative real-time PCR

Viral DNA replication was assayed by real-time PCR, as previously described (Vanarsdall et al., 2004) with modifications. To prepare total DNA for analysis, *Sf*9 cells (1.0×10^6 cells/35 mm-diameter well of a six-well plate) were transfected with 1.0 μg of bacmid DNA (AcBAC$^{ac142\text{REP-}ac143\text{KO}}$, AcBAC$^{ac142\text{REP-}ac143\text{REP}}$, AcBAC$^{ac142\text{REP-}ac143(1\ \text{TAAG})}$, AcBAC$^{ac142\text{REP-}ac143(2\ \text{TAAG})}$, AcBAC$^{ac142\text{REP-}ac143(3\ \text{TAAG})}$, AcBAC$^{ac142\text{REP-}ac143(3\ \text{TAAG+UP})}$ or AcBAC$^{\text{PH-GFP}}$) and at designated times post-transfection, cells were washed once with 1× phosphate-buffered saline (1× PBS, 137 mM NaCl, 10 mM Phosphate, 2.7 mM KCl, pH 7.4), scraped with a rubber policeman and pelleted (8000 ×*g* for 5 min). Each pellet was resuspended in 1 ml of 0.4 M NaOH–125 mM EDTA and incubated at 100 °C for 10 min to disrupt the cells. An aliquot of the lysed cells (50 μl) was treated with 250 μl Tris–HCl pH 7.5 and 20 μg/ml RNAse A at 37 °C for 30 min before adding 80 μg/ml Proteinase K and incubating overnight at 50 °C. Total DNA was extracted with 300 μl of phenol-chloroform and 300 μl of chloroform; and a 50 μl aliquot was then carefully removed from the aqueous layer. Prior to the PCR, 2 μl of total DNA from each time-point was digested with 40 U of *Dpn*I restriction enzyme (New England Biolabs) overnight in a 20 μl total reaction volume. An aliquot of the digested DNA (2 μl) was combined with the New England Biolabs SYBR Master Mix (DyNAmo

HS SYBR Green qPCR Kit) and the qPCR primers 1483 (5′-CGTAGTGGTAGTAATCGCCGC-3′) and 1484 (5′-AGTCGAGTCGCGTCGCTTT-3′) in a 20 μl reaction. The samples were analyzed in a Stratagene MX4000 qPCR cycler under the following conditions: 1 cycle of 95 °C for 15 min; 40 cycles of 95 °C for 30 s, 52 °C for 24 s, 72 °C for 30 s; 1 cycle of 95 °C for 1 min; 41 cycles of 55 °C for 30 s. The results were analyzed using Stratagene MX4000 software.

Transcriptional analysis of ac143

For the synthesis of a single-stranded RNA Northern blot probe homologous to *ac143*, a 183-nt fragment was PCR amplified from within the *ac143* ORF with upper primer 1487 (5′-CCATCTTGGCTGTAGTAGTAATTATTGC-3′) and lower primer 1488 (5′-TCA*TAATACGACTCACTATAGGG*G-GCGTGTTCATAAAGGGATTAG-3′), which incorporated the T7 promoter (sequence in italics). AcMNPV-E2 DNA as used as the PCR template. This fragment was gel purified and used to generate an RNA probe using T7 RNA polymerase by standard methods (Sambrook and Russell, 2001).

RNA was extracted from *Sf*9 cells (1.0×10^6/35-mm-diameter six-well plate) transfected with 1.0 μg of bacmid DNA (AcBAC$^{ac142\text{REP-}ac143\text{KO}}$, AcBAC$^{ac142\text{REP-}ac143(1\ \text{TAAG})}$, AcBAC$^{ac142\text{REP-}ac143(2\ \text{TAAG})}$, AcBAC$^{ac142\text{REP-}ac143(3\ \text{TAAG})}$, AcBAC$^{ac142\text{REP-}ac143(3\ \text{TAAG+UP})}$ or AcBAC$^{\text{PH-GFP}}$) at designated times post-infection. RNA from each time-point was isolated using RNeasy mini-kit (QIAGEN Cat. No.12462). Total RNA (5 μg) was separated by electrophoresis on a 1.25% formaldehyde gel, blotted (Fourney et al., 1988) and hybridized with a α-^{32}P-radiolabled *ac143* probe (Sambrook and Russell, 2001). The blot was visualized by exposure to Perkin Elmer Multisensitive Phosphorscreens, scanned using a Cyclone PhosphorImager (Perkin Elmer) and analyzed with Optiquant Acquisition and Analysis Software V5.0 (Perkin Elmer).

Note added in proof

The online Viral Bioinformatics Resource Center (http://athena.bioc.uvic.ca/) has also identified the CuniNPV ORF *cuni31* as a gene common to all sequenced baculovirus genomes.

Acknowledgments

We give special thanks to Les Willis for his excellent technical support. This study was supported by the Canadian Crop Genomics Initiative from Agriculture and Agri-Food Canada.

References

Afonso, C.L., Tulman, E.R., Lu, Z., Balinsky, C.A., Moser, B.A., Becnel, J.J., Rock, D.L., Kutish, G.F., 2001. Genome sequence of a baculovirus pathogenic for *Culex nigripalpus*. J. Virol. 75, 11157–11165.

Ayres, M.D., Howard, S.C., Kuzio, J., Lopez-Ferber, M., Possee, R.D., 1994. The complete DNA sequence of *Autographa californica* nuclear polyhedrosis virus. Virology 202, 586–605.

Braunagel, S.C., He, H., Ramamurthy, P., Summers, M.D., 1996. Transcription, translation, and cellular localization of three *Autographa californica* nuclear polyhedrosis virus structural proteins: ODV-E18, ODV-E35, and ODV-EC27. Virology 222, 100–114.

Dai, X., Stewart, T.M., Pathakamuri, J.A., Li, Q., Theilmann, D.A., 2004. *Autographa californica* multiple nucleopolyhedrovirus exon0 (*orf*141), which encodes a RING finger protein, is required for efficient production of budded virus. J. Virol. 78, 9633–9644.

Datsenko, K.A., Wanner, B.L., 2000. One-step inactivation of chromosomal genes in *Escherichia coli* K-12 using PCR products. Proc. Natl. Acad. Sci. U. S. A. 97, 6640–6645.

Duffy, S.P., Young, A.M., Morin, B., Lucarotti, C.J., Koop, B.F., Levin, D.B., 2006. Sequence analysis and organization of the *Neodiprion abietis* nucleopolyhedrovirus genome. J. Virol. 80, 6952–6963.

Fourney, R.M., Day III, R.S., Paterson, M.C., 1988. Northern blotting: efficient RNA staining and transfer. Focus 10, 5–7.

Garcia-Maruniak, A., Maruniak, J.E., Zanotto, P.M., Doumbouya, A.E., Liu, J.C., Merritt, T.M., Lanoie, J.S., 2004. Sequence analysis of the genome of the *Neodiprion sertifer* nucleopolyhedrovirus. J. Virol. 78, 7036–7051.

Granados, R.R., Lawler, K.A., 1981. In vivo pathway of *Autographa californica* baculovirus invasion and infection. Virology l08, 297–308.

Harrison, R.L., Bonning, B.C., 2003. Comparative analysis of the genomes of *Rachiplusia ou* and *Autographa californica* multiple nucleopolyhedroviruses. J. Gen. Virol. 84, 1827–1842.

Herniou, E.A., Olszewski, J.A., Cory, J.S., O'Reilly, D.R., 2003. The genome sequence and evolution of baculoviruses. Annu. Rev. Entomol. 48, 211–234.

Hou, S., Chen, X., Wang, H., Tao, M., Hu, Z., 2002. Efficient method to generate homologous recombinant baculovirus genomes in *E. coli*. Biotechniques 32, 783–788.

Jehle, J.A., Blissard, G.W., Bonning, B.C., Cory, J.S., Herniou, E.A., Rohrmann, G.F., Theilmann, D.A., Thiem, S.M., Vlak, J.M., 2006. On the classification and nomenclature of baculoviruses: a proposal for revision. Arch. Virol. 151, 1257–1266.

Keddie, B.A., Aponte, G.W., Volkman, L.E., 1989. The pathway of infection of *Autographa californica* nuclear polyhedrosis virus in an insect host. Science 243, 1728–1730.

Kovacs, G.R., Guarino, L.A., Graham, B.L., Summers, M.D., 1991. Identification of spliced baculovirus RNAs expressed late in infection. Virology 185, 633–643.

Lauzon, H.A., Lucarotti, C.J., Krell, P.J., Feng, Q., Retnakaran, A., Arif, B.M., 2004. Sequence and organization of the *Neodiprion lecontei* nucleopolyhedrovirus genome. J. Virol. 78, 7023–7035.

Lauzon, H.A., Garcia-Maruniak, A., Zanotto, P.M., Clemente, J.C., Herniou, E.A., Lucarotti, C.J., Arif, B.M., Maruniak, J.E., 2006. Genomic comparison of *Neodiprion sertifer* and *Neodiprion lecontei* nucleopolyhedroviruses and identification of potential hymenopteran baculovirus-specific open reading frames. J. Gen. Virol. 87, 1477–1489.

Lee, H.H., Miller, L.K., 1979. Isolation, complementation, and initial characterization of temperature-sensitive mutants of the baculovirus *Autographa californica* nuclear polyhedrosis virus. J. Virol. 31, 240–252.

Lin, G., Blissard, G.W., 2002. Analysis of an *Autographa californica* multicapsid nucleopolyhedrovirus lef-6-null virus: LEF-6 is not essential for viral replication but appears to accelerate late gene transcription. J. Virol. 76, 5503–5514.

Lo, H.R., Chao, Y.C., 2004. Rapid titer determination of baculovirus by quantitative real-time polymerase chain reaction. Biotechnol. Prog. 20, 354–360.

Luckow, V.A., Lee, S.C., Barry, G.F., Olins, P.O., 1993. Efficient generation of infectious recombinant baculoviruses by site-specific transposon-mediated insertion of foreign genes into a baculovirus genome propagated in *Escherichia coli*. J. Virol. 67, 4566–4579.

Lung, O.Y., Cruz-Alvarez, M., Blissard, G.W., 2003. Ac23, an envelope fusion protein homolog in the baculovirus *Autographa californica* multicapsid nucleopolyhedrovirus, is a viral pathogenicity factor. J. Virol. 77, 328–339.

McCarthy, C.B., Dai, X., Donly, C., Theilmann, D.A., 2008. *Autographa californica* multiple nucleopolyhedrovirus *ac142*, a core gene that is essential for BV production and ODV envelopment. Virology 372, 325–339.

Olszewski, J., Miller, L.K., 1997a. Identification and characterization of a baculovirus structural protein, VP1054, required for nucleocapsid formation. J. Virol. 71, 5040–5050.

Olszewski, J., Miller, L.K., 1997b. A role of baculovirus GP41 in budded virus production. Virology. 233, 292–301.

Possee, R.D., Sun, T.P., Howard, S.C., Ayres, M.D., Hill Perkins, M., Gearing, K.L., 1991. Nucleotide sequence of the *Autographa californica* nuclear polyhedrosis 9.4 kbp *Eco*RI-I and R polyhedrin gene region. Virology 185, 229–241.

Russell, R.L.Q., Funk, C.J., Rohrmann, G.F., 1997. Association of a baculovirus-encoded protein with the capsid basal region. Virology 227, 142–152.

Sambrook, J., Russell, D.W., 2001. Molecular Cloning: A Laboratory Manual, 3rd ed. Cold Spring Harbor Laboratory Press, Cold Spring Harbor, N.Y. (3 vols.).

Stewart, T.M., Huijskens, I., Willis, L.G., Theilmann, D.A., 2005. The *Autographa californica* multiple nucleopolyhedrovirus ie0–ie1 gene complex is essential for wild-type virus replication, but either IE0 or IE1 can support virus growth. J. Virol. 79, 4619–4629.

Theilmann, D.A., Blissard, G.W., Bonning, B., Jehle, J., O'Reilly, D.R., Rohrmann, G.F., Thiem, S., Vlak, J.M., 2005. *Baculoviridae*. In: Van Regenmortel, H.V., Bishop, D.H.L., Van Regenmortel, M.H., Fauquet, C.M. (Eds.), Virus Taxonomy: Eighth Report of the International Committee on Taxonomy of Viruses. Elsevier Academic Press, New York, pp. 177–185.

Vanarsdall, A.L., Okano, K., Rohrmann, G.F., 2004. Characterization of a baculovirus with a deletion of *vlf*-1. Virology 326, 191–201.

Vanarsdall, A.L., Okano, K., Rohrmann, G.F., 2006. Characterization of the role of very late expression factor 1 in baculovirus capsid structure and DNA processing. J. Virol. 80, 1724–1733.

Vanarsdall, A.L., Pearson, M.N., Rohrmann, G.F., 2007. Characterization of baculovirus constructs lacking either the Ac 101, Ac 142, or the Ac 144 open reading frame. Virology 367, 187–195.

Vialard, J.E., Richardson, C.D., 1993. The 1629-nucleotide open reading frame located downstream of the *Autographa californica* nuclear polyhedrosis virus polyhedrin gene encodes a nucleocapsid-associated phosphoprotein. J. Virol. 67, 5859–5866.

Wu, W., Lin, T., Pan, L., Yu, M., Li, Z., Pang, Y., Yang, K., 2006. *Autographa californica* multiple nucleopolyhedrovirus nucleocapsid assembly is interrupted upon deletion of the 38 K gene. J. Virol. 80, 11475–11485.

Yang, S., Miller, L.K., 1998. Expression and mutational analysis of the baculovirus very late factor 1 (*vlf-1*) gene. Virology 245, 99–109.